FLOW INDUCED VIBRATION OF AN AIRFOIL WITH THREE DEGREES OF FREEDOM

Martin Růžička, Miloslav Feistauer
Charles University Prague, Faculty of Mathematics and Physics, Sokolovská 83, 186 75 Praha 8, Czech Republic

Jaromír Horáček
Academy of Sciences of the Czech Republic, Institute of Thermomechanics, Dolejškova 5, 182 00 Praha 8, Czech Republic

Petr Sváček
Czech Technical University Prague, Faculty of Mechanical Engineering, Karlovo n. 13, 121 35 Praha 2, Czech RepublicKarlovo n. 13, 121 35 Praha 2, Czech Republic

ABSTRACT

The subject of this article is the numerical simulation of the interaction of two-dimensional incompressible viscous fluid and a vibrating airfoil with large amplitudes. A solid airfoil with three degrees of freedom can rotate around the elastic axis, oscillate in the vertical direction and its flap can rotate. The numerical simulation consists of the finite element solution of the Navier-Stokes equations coupled with a system of nonlinear ordinary differential equations describing the airfoil motion. The time-dependent computational domain and a moving grid are taken into account with the aid of the Arbitrary Lagrangian-Eulerian (ALE) formulation. High Reynolds numbers up to 10^6 *require the application of a suitable stabilization of the finite element discretization. Numerical tests and comparison with NASTRAN solver prove that the developed method is sufficiently accurate and robust.*

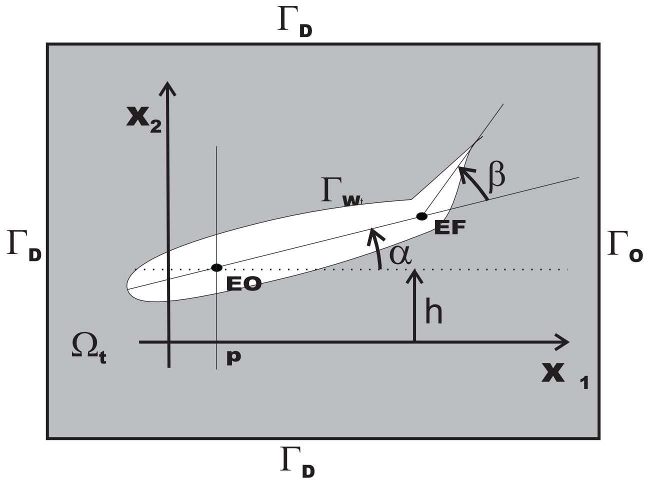

Figure 1: *Schema of an airfoil with 3 degrees of freedom.*

1. INTRODUCTION

The interaction of fluids and structures plays an important role in many fields of science and technology. The aeroelastic stability of aerospace vehicles and the aeroelastic responses represented by dynamic load prediction and vibration levels in wings, tails and other aerodynamic surfaces have a great impact on the design as well as in the cost and operational safety. We paid attention to several aspects of the numerical simulation of flow induced vibrations. In Sváček at al (2007) we analyzed numerically the interaction of a moving fluid with an isolated airfoil. In many cases it is necessary to compare computational results with wind tunnel experiments. This is the subject of the paper Feistauer at al (2007), where the flow induced vibrations were analyzed numerically for an airfoil with two degrees of freedom, inserted in a channel (wind tunnel). In this case the airfoil can ocsillate in the vertical direction and rotate around an elastic axis. In the present paper we are concerned with interaction of a moving fluid and an airfoil with three degrees of freedom, see Fig.1. This means that the airfoil is formed by two parts - the main part and a flap. The degrees of freedom are the vertical displacement, the rotation of the complete configuration around the main elastic axis and the rotation of the flap around the flap elastic axis. Computational results were obtained for the airfoil NACA0012 inserted in a channel.

2. MATHEMATICAL MODEL

2.1. ALE formulation of the Navier-Stokes equations

The ALE description is given by a smooth, one to one mapping

$$\mathbf{A}_t : \Omega_0 \mapsto \Omega_t, \quad \mathbf{X} \mapsto \mathbf{x}(\mathbf{X}, t) = \mathbf{A}_t(\mathbf{X}), \tag{1}$$

(defined for each $t \in I = [0, T]$) of the reference domain Ω_0 onto the domain Ω_t. The mapping $\mathbf{A}_t$ is identical in the vicinity of the part of the boundary, which is not deformed. The coordinates of a point $\mathbf{x}$ are spatial coordinates, coordinates of a point $\mathbf{X}$ are ALE or reference coordinates.

First, we define the domain velocity

$$\tilde{\mathbf{w}}(\mathbf{X}, t) = \frac{\partial}{\partial t}\mathbf{x}(\mathbf{X}, t). \tag{2}$$

This velocity can be expressed in spatial coordinates as

$$\mathbf{w}(\mathbf{x}, t) = \tilde{\mathbf{w}}(\mathbf{A}_t^{-1}(\mathbf{x}), t). \tag{3}$$

Let us consider a function $f : M \mapsto \mathrm{R}$, where R is the set of all real numbers and $M = \{(t, \mathbf{x});\ t \in I, \mathbf{x} \in \Omega_t\}$, and denote $\tilde{f}(\mathbf{X}, t) = f(\mathbf{A}_t(\mathbf{X}), t)$. Then we define the ALE derivative of f by

$$\frac{D^A}{Dt} f : M \mapsto \mathrm{R}, \quad \frac{D^A}{Dt} f(\mathbf{x}, t) = \frac{\partial \tilde{f}}{\partial t}(\mathbf{X}, t)$$

$$\mathbf{X} = \mathbf{A}_t^{-1}(\mathbf{x}). \tag{4}$$

The application of the chain rule gives

$$\frac{D^A}{Dt}\mathbf{f} = \frac{\partial \mathbf{f}}{\partial t} + (\mathbf{w} \cdot \nabla)\mathbf{f}. \tag{5}$$

Using this relation, we can obtain the Navier-Stokes equations in the ALE form

$$\frac{D^A}{Dt}\mathbf{u} + [(\mathbf{u} - \mathbf{w}) \cdot \nabla]\mathbf{u} + \nabla p - \nu \triangle \mathbf{u} = 0 \quad \text{in } \Omega_t$$

$$\operatorname{div} \mathbf{u} = 0 \quad \text{in } \Omega_t. \tag{6}$$

The solution of these equations characterizes the flow by the velocity field $\mathbf{u} = \mathbf{u}(x, t)$ and the kinematic pressure $p = p(x, t)$, $x \in \Omega_t$ and $t \in [0, T]$.

2.1.1. *Equations of motion of the airfoil*

The equations for moving profile with 3 degrees of freedom are derived from the Euler-Lagrange equations for generalized coordinates h-vertical displacement, α-torsion around the main elastic axis EO and β-the torsion of the flap around the flap elastic axis EF. The equations have the form

$$\begin{aligned}
&m\ddot{h} + [(S_\alpha - S_\beta)\cos\alpha + S_\beta \cos(\alpha + \beta)]\ddot{\alpha} \\
&+S_\beta \cos(\alpha + \beta)\ddot{\beta} - (S_\alpha - S_\beta)\sin\alpha\dot{\alpha}^2 \\
&-S_\beta \sin(\alpha + \beta)(\dot{\alpha} + \dot{\beta})^2 + D_{hh}\dot{h} + k_{hh}h = L_2 \\
&[(S_\alpha - S_\beta)\cos\alpha + S_\beta\cos(\alpha + \beta)]\ddot{h} \\
&+[(I_\alpha - 2x_{1T}S_\beta) + 2x_{1T}S_\beta\cos\beta]\ddot{\alpha} \\
&+[I_\beta + x_{1T}S_\beta\cos\beta]\ddot{\beta} - x_{1T}S_\beta\sin\beta\dot{\beta}^2 \\
&-2x_{1T}S_\beta\sin\beta\dot{\alpha}\dot{\beta} + D_{\alpha\alpha}\dot{\alpha} + k_{\alpha\alpha}\alpha = M_\alpha \\
&S_\beta\cos(\alpha + \beta)\ddot{h} + [I_\beta + x_{1T}S_\beta\cos\beta]\ddot{\alpha} + I_\beta\ddot{\beta} \\
&+x_{1T}S_\beta\sin\beta\dot{\alpha}^2 + D_{\beta\beta}\dot{\beta} + k_{\beta\beta}\beta = M_\beta.
\end{aligned} \tag{7}$$

Here m is the mass of the entire airfoil, S_α is the static moment with respect to the axis EO, S_β is the static moment of the flap section with respect to the axis EF, I_α is the inertia moment with respect to the axis EO, I_β is the inertia moment of the flap section with respect to the axis EF. The constants D_{hh}, $D_{\alpha\alpha}$, $D_{\beta\beta}$ are aerodynamical damping coefficients and k_{hh}, $k_{\alpha\alpha}$, $k_{\beta\beta}$ are stiffness coefficients. The constant x_{1T} is distance between EO and EF. The forces are represented by L_2, M_α, M_β, which mean vertical force, the momentum of the force on the entire airfoil with respect to the main elastic axis EO and the momentum of the force on the flap section with respect to the flap elastic axis EF.

The linearized equations in the matrix form read

$$\widehat{\boldsymbol{K}}\boldsymbol{d}(t) + \widehat{\boldsymbol{B}}\dot{\boldsymbol{d}}(t) + \widehat{\boldsymbol{M}}\ddot{\boldsymbol{d}}(t) = \widehat{\boldsymbol{f}}(t), \tag{8}$$

where the stiffness matrix $\widehat{\boldsymbol{K}}$, the viscous damping $\widehat{\boldsymbol{B}}$ and the mass matrix $\widehat{\boldsymbol{M}}$ have the form

$$\widehat{\boldsymbol{K}} = \begin{pmatrix} k_{hh} & 0 & 0 \\ 0 & k_{\alpha\alpha} & 0 \\ 0 & 0 & k_{\beta\beta} \end{pmatrix},$$

$$\widehat{\boldsymbol{B}} = \begin{pmatrix} D_{hh} & 0 & 0 \\ 0 & D_{\alpha\alpha} & 0 \\ 0 & 0 & D_{\beta\beta} \end{pmatrix},$$

$$\widehat{\boldsymbol{M}} = \begin{pmatrix} m & S_\alpha & S_\beta \\ S_\alpha & I_\alpha & I_\beta + x_{1T}S_\beta \\ S_\beta & I_\beta + x_{1T}S_\beta & I_\beta \end{pmatrix}.$$

The vector of the force $\widehat{\boldsymbol{f}}$ and the vector of the generalized coordinates $\boldsymbol{d}$ are given by

$$\widehat{\boldsymbol{f}}(t) = \begin{pmatrix} L_2(t) \\ \mathcal{M}_\alpha(t) \\ \mathcal{M}_\beta(t) \end{pmatrix}, \quad \boldsymbol{d} = \begin{pmatrix} h(t) \\ \alpha(t) \\ \beta(t) \end{pmatrix}.$$

2.2. Initial and boundary conditions

The Navier-Stokes equations are completed by the initial condition

$$\boldsymbol{u}(x,0) = \boldsymbol{u}_0, \quad x \in \Omega_0, \tag{9}$$

and boundary conditions. The part of the boundary Γ_D represents the inlet and impermeable fixed walls. On Γ_D we specify the Dirichlet boundary condition

$$\boldsymbol{u}|_{\Gamma_D} = \boldsymbol{u}_D. \tag{10}$$

The part of the boundary Γ_O is the outlet, where we use the so-called do-nothing boundary condition

$$-(p - p_{ref})\,\boldsymbol{n} + \nu \frac{\partial \boldsymbol{u}}{\partial \boldsymbol{n}} = 0 \quad \text{on } \Gamma_O, \tag{11}$$

where p_{ref} is a given reference pressure. On Γ_{W_t}, representing the surface of the airfoil, we consider the condition

$$\boldsymbol{u}|_{\Gamma_{W_t}} = \widetilde{\boldsymbol{u}}|_{W_t} = \boldsymbol{w}|_{\Gamma_{W_t}}. \tag{12}$$

Moreover, we use the initial conditions for system (7) or (8)

$$\begin{aligned} &\alpha(0) = \alpha_0,\ \dot{\alpha}(0) = \alpha_1, \\ &\beta(0) = \beta_0,\ \dot{\beta}(0) = \beta_1, \\ &h(0) = h_0,\ \dot{h}(0) = h_1, \end{aligned} \tag{13}$$

where α_0, α_1, β_0, β_1, h_0, h_1 are given constants.

3. DISCRETIZATION OF THE PROBLEM

3.1. Time discretization

We use an equidistant partition of the time interval $[0,T]$, formed by $0 = t_0 < t_1 < \cdots < T$, $t_k = k\tau$, where $\tau > 0$ is a time step, and apply a three point backward difference scheme. On each time level t_{n+1} we obtain the problem to find functions $\boldsymbol{u}^{n+1} : \Omega_{t_{n+1}} \mapsto I\!R^2$ and $p^{n+1} : \Omega_{t_{n+1}} \mapsto I\!R$ such that

$$\begin{aligned} &\frac{3\boldsymbol{u}^{n+1} - 4\hat{\boldsymbol{u}}^n + \hat{\boldsymbol{u}}^{n-1}}{2\tau} \\ &+ \Big((\boldsymbol{u}^{n+1} - \boldsymbol{w}^{n+1}) \cdot \nabla \Big) \boldsymbol{u}^{n+1} \\ &-\nu \Delta \boldsymbol{u}^{n+1} + \nabla p^{n+1} = 0 \quad \text{in } \Omega_{t_{n+1}}, \\ &\operatorname{div} \boldsymbol{u}^{n+1} = 0 \quad \text{in } \Omega_{t_{n+1}}. \end{aligned} \tag{14}$$

Here $\boldsymbol{u}^k$, p^k and $\boldsymbol{w}^k$ denote the approximations of the functions $\boldsymbol{u}(t_k)$, $p(t_k)$ and $\boldsymbol{w}(t_k)$, respectively.

This system is considered with the boundary conditions (10), (11), (12). The symbols $\hat{\boldsymbol{u}}^n$ and $\hat{\boldsymbol{u}}^{n-1}$ mean the functions $\boldsymbol{u}^n$ and $\boldsymbol{u}^{n-1}$ transformed from the domain Ω_{t_n} and $\Omega_{t_{n-1}}$ to the domain $\Omega_{t_{n+1}}$ using the ALE mapping.

3.2. Discretization in space

The starting point for the space discretization is the weak formulation of problem (14). For this purpose we introduce a simplified notation $\Omega = \Omega_{t_{n+1}}, \boldsymbol{u} = \boldsymbol{u}^{n+1}, p = p^{n+1}$ and use the appropriate function spaces $W = (H^1(\Omega))^2$ (the Sobolev space), $X = \{\mathbf{v} \in W;\, \mathbf{v}|_{\Gamma_D \cup \Gamma_{W_t}} = 0\}$ and $M = L^2(\Omega)$. We introduce the notation

$$\begin{aligned} a(U^*, U, V) = \frac{3}{2\tau}(\boldsymbol{u}, \boldsymbol{v}) + \\ \nu((\boldsymbol{u}, \boldsymbol{v})) + (((\boldsymbol{u}^* - \boldsymbol{w}^{n+1}) \cdot \nabla)\, \boldsymbol{u}, \boldsymbol{v}) \\ -(p,\, \nabla \cdot \boldsymbol{v}) + (\nabla \cdot \boldsymbol{u},\, q), \end{aligned} \tag{15}$$

$$f(V) = \frac{1}{2\tau}\Big(4\hat{\boldsymbol{u}}^n - \hat{\boldsymbol{u}}^{n-1},\, \boldsymbol{v}\Big) - \int_{\Gamma_O} \boldsymbol{v} \cdot \boldsymbol{n} \, \mathrm{d}s,$$

where

$$(a, b) = \int_\Omega ab \, \mathrm{d}x$$

and

$$U = (\boldsymbol{u}, p) \in W \times M$$

$$U^* = (\boldsymbol{u}^*, p) \in W \times M$$

$$V = (\boldsymbol{v}, q) \in X \times M.$$

The solution of the weak formulation is $U = (\mathbf{u}, p)$ such that it satisfies the conditions

$$\begin{aligned} U \in W \times M, \quad a(U, U, V) = f(V) \\ \forall V = (\mathbf{v}, q) \in X \times M, \end{aligned} \tag{16}$$

and $\mathbf{u}$ satisfies the boundary conditions (10) and (12).

In the finite element approximation we approximate the spaces W, X, M by their finite-dimensional subspaces $W_\Delta, X_\Delta, M_\Delta$, $\Delta \in (0, \Delta_0)$, $\Delta_0 > 0$, where

$$X_\Delta = \left\{ \boldsymbol{v} \in W_\Delta;\, \boldsymbol{v}|_{\Gamma_D \cup \Gamma_{W_t}} = 0 \right\}.$$

This means that for each $\Delta \in (0, \Delta_0)$ we assign finite dimensional subspaces W_Δ, X_Δ, M_Δ, with dimensions $\dim W_\Delta = n_W(\Delta)$, $\dim X_\Delta = n_X(\Delta)$, $\dim M_\Delta = n_M(\Delta)$. The approximate solution is defined as a couple $U_\Delta = (\boldsymbol{u}_\Delta, p_\Delta) \in W_\Delta \times M_\Delta$ such that

$$a(U_\Delta, U_\Delta, V_\Delta) = f(V_\Delta),$$
$$\forall\, V_\Delta = (\boldsymbol{v}_\Delta, q_\Delta) \in X_\Delta \times M_\Delta \qquad (17)$$

and $\boldsymbol{u}_\Delta$ satisfies an approximation of the boundary conditions (10) and (12). The finite element spaces X_Δ and M_Δ must satisfy the Babuška-Brezzi (BB) condition, which guarantees the stability of the used scheme. In our computations we use the well-known Taylor-Hood P^2/P^1 elements satisfying the (BB) condition (Brezzi and Falk (1991)).

4. CONSTRUCTION OF THE ALE MAPPING

To perform the deformation of the computational domain in the ALE formulation, we must construct the ALE mapping numerically. We define it via the solution of the linear elasticity equations

$$(\lambda + \mu)\nabla \operatorname{div} \boldsymbol{g} + \mu \Delta \boldsymbol{g} = 0 \in \Omega_0, \qquad (18)$$

where λ and μ are Lamé coefficients and $\boldsymbol{g}$ is defined in the domain Ω_0. Boundary conditions for $\boldsymbol{g}$ are prescribed by $\boldsymbol{g}|_{\Gamma_D \cup \Gamma_O} = 0$ and $\boldsymbol{g}|_{\Gamma_{W_0}}$ is computed from the motion of the airfoil, which is given for each time t by $\alpha(t)$, $\beta(t)$, $h(t)$. Solving equation (18) gives the ALE mapping of the domain Ω_0 onto Ω_t by the relations $\boldsymbol{A}_t : \boldsymbol{X} \mapsto x(\boldsymbol{X}, t) = \boldsymbol{A}_t(\boldsymbol{X}) = \boldsymbol{X} + \boldsymbol{g}$ for each time instant t. Then, from this field we construct the domain velocity $\boldsymbol{w}$ used in (6).

5. STABILIZATION OF THE FINITE ELEMENT METHOD

In order to get correct and accurate results, it is necessary to apply the stabilization of the finite element method. The reason is that the standard application of the finite element method leads to

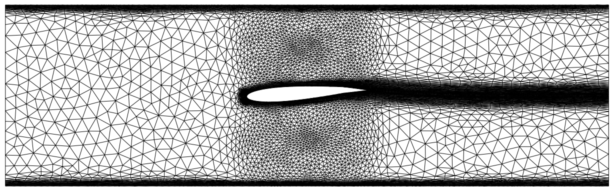

Figure 2: *ALE linear elastic deformation of the anisotropically adapted mesh for NACA0012 with $h = 0mm$, $\alpha = 4^0$, $\beta = -4^0$ and EO in 33.33% and EF in 80% of the profile chord.*

numerical schemes that give non-physical results represented by spurious oscillations, which appear in the computed solution in the case of high Reynolds numbers.

In our case we apply the streamline diffusion method analyzed in Gelhard at al (2005). We have the triangulation $\mathcal{T}_\Delta$ of the domain $\Omega = \Omega_{t_{n+1}}$ with triangles K. We define the stabilization forms

$$\begin{aligned} & L_\Delta(U^*, U, V) \\ & = \sum_{K \in \mathcal{T}_\Delta} \delta_K \left(\frac{3}{2\tau}\boldsymbol{u} - \nu \Delta \boldsymbol{u} \right. \\ & \left. + (\overline{\boldsymbol{w}} \cdot \nabla)\, \boldsymbol{u} + \nabla p, (\overline{\boldsymbol{w}} \cdot \nabla)\, \boldsymbol{v} \right)_K, \qquad (19) \\ & F_\Delta(V) \\ & = \sum_{K \in \mathcal{T}_\Delta} \delta_K \left(\frac{1}{2\tau}(4\widehat{\boldsymbol{u}}^n - \widehat{\boldsymbol{u}}^{n-1}),\, (\overline{\boldsymbol{w}} \cdot \nabla)\, \boldsymbol{v} \right)_K, \end{aligned}$$

where

$$U = (\boldsymbol{u}, p) \quad U^* = (\boldsymbol{u}^*, p) \quad V = (\boldsymbol{v}, q),$$

$\delta_K \geq 0$ are suitable parameters, $\overline{\boldsymbol{w}} = \boldsymbol{u}^* - \boldsymbol{w}^{n+1}$ is the transport velocity and $(\cdot, \cdot)_K$ is the scalar product in the space $L^2(K)$.

Moreover, we define the stabilization pressure form

$$P_\Delta(U, V) = \sum_{K \in \mathcal{T}_\Delta} \tau_K (\nabla \cdot \boldsymbol{u},\, \nabla \cdot \boldsymbol{v})_K,$$
$$U = (\boldsymbol{u}, p) \quad V = (\boldsymbol{v}, q), \qquad (20)$$

with suitable parameters $\tau_K \geq 0$.

The solution of the stabilized discrete problem is $U_\Delta = (\boldsymbol{u}_\Delta, p_\Delta) \in W_\Delta \times M_\Delta$ such that the component $\boldsymbol{u}_\Delta$ satisfies the boundary conditions (10) on Γ_D and (12) on Γ_{W_t} and

$$a_\Delta(U_\Delta, U_\Delta, V_\Delta) + L_\Delta(U_\Delta, U_\Delta, V_\Delta)$$
$$+ P_\Delta(U_\Delta, V_\Delta) = f_\Delta(V_\Delta) + F_\Delta(V_\Delta), \qquad (21)$$
$$\forall\, V_\Delta = (\boldsymbol{v}_\Delta, q_\Delta) \in X_\Delta \times M_\Delta.$$

Now, we describe the choice of the δ_K and τ_K. We split the computational domain into two subdomains. The diffusion component dominates in the first subdomain and the convective component dominates in the second one. In both subdomains we choose these parameters in a different way. The definition of the parameters δ_K is based on the transport velocity $\overline{\boldsymbol{w}}$ and the viscosity ν. We put

$$\delta_K = \delta^* \frac{\Delta_K}{2\|\overline{\boldsymbol{w}}\|_{L^\infty(K)}} \, \xi(\Re^{\overline{\boldsymbol{w}}}), \tag{22}$$

where

$$\Re^{\overline{\boldsymbol{w}}} = \frac{\delta_K \|\overline{\boldsymbol{w}}\|_{L^\infty(K)}}{2\nu} \tag{23}$$

is the so-called local Reynolds number and Δ_K is the size of the element K measured in the direction of $\overline{\boldsymbol{w}}$. The function $\xi(\cdot)$ is non-decreasing in dependence on $\Re^{\overline{\boldsymbol{w}}}$ in such a way, that for local convective dominance ($\Re^{\overline{\boldsymbol{w}}} > 1$) $\xi \to 1$ and for local diffusion dominance ($\Re^{\overline{\boldsymbol{w}}} < 1$) $\xi \to 0$. The parameter δ is chosen as an element of the interval $(0, 1]$. The function $\xi(\cdot)$ can be defined in the form

$$\xi(\Re^{\overline{\boldsymbol{w}}}) = \min\left(\frac{\Re^{\overline{\boldsymbol{w}}}}{6}, 1\right). \tag{24}$$

The parameters τ_K are defined by

$$\tau_K = \tau^* \Delta_K \|\overline{\boldsymbol{w}}\|_{L^\infty(K)} \quad \text{and} \quad \tau_K = 0 \tag{25}$$

for local convective dominance and local diffusion dominance, respectively, and $\tau^* \in (0, 1]$.

6. RESULTS

Here we present the results comparable with a linear frequency-model and stability analysis performed by Losík and Čečrdle (2007) using the NASTRAN code for the 0% balanced flap. We considered NACA0012 airfoil with chord lenght c=0.3 m, axis EO at c/3 and axis EF at 0,8 c. The numerical simulation was carried out for the following data:
$m = 0.086622\,\text{kg}$, $k_{hh} = 105.109\,\text{N/m}$,
$k_{\alpha\alpha} = 3.69558\,\text{N rad/m}$, $k_{\beta\beta} = 0.2\,\text{N rad/m}$,
$S_\alpha = 0.000779598\,\text{kg m}$, $S_\beta = 0\,\text{kg m}$,
$I_\alpha = 0.000487291\,\text{kg m}^2$, $x_{1T} = 0.14\,\text{m}$,
$I_\beta = 0.0000341104\,\text{kg m}^2$, $D_{hh} = 0\,\text{Ns/m}$,
$D_{\alpha\alpha} = 0\,\text{Ns rad/m}$, $D_{\beta\beta} = 0\,\text{Ns rad/m}$.
Examples of computed free airfoil vibrations are presented in Figs. 3 and 4 for two inlet airflow velocities. The translational and rotational vibration amplitudes for the flow velocity 5 m/s

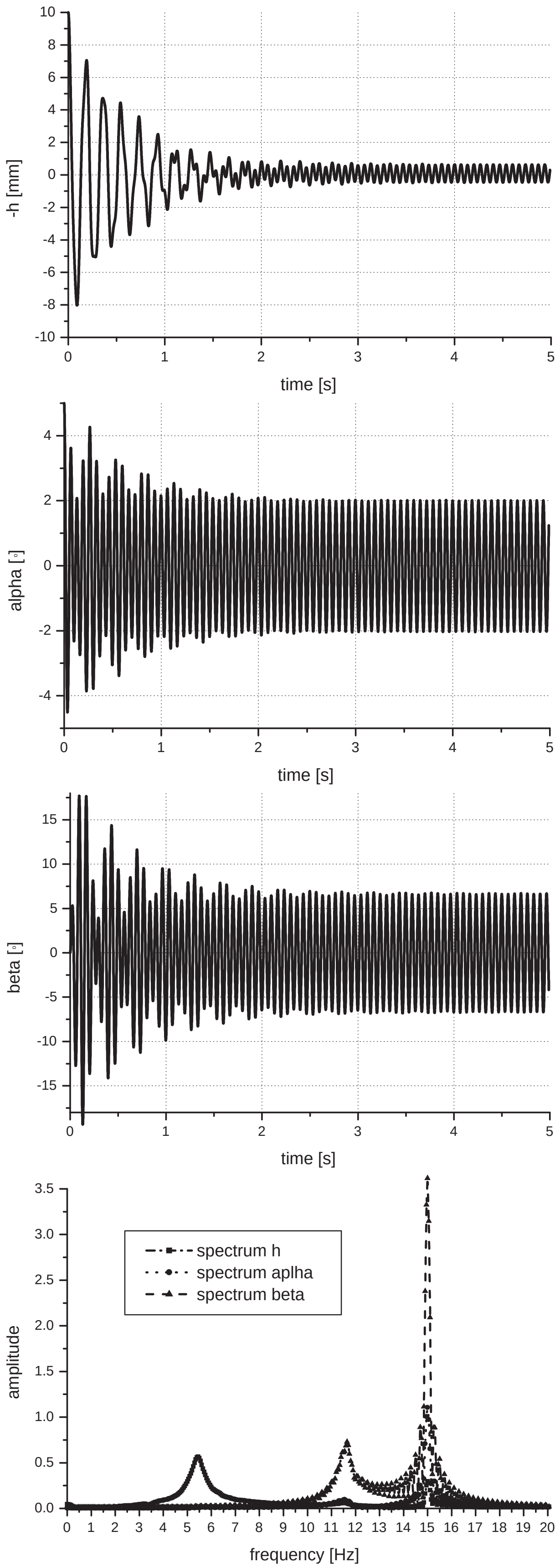

Figure 3: *Functions h, α, β and their spectral analysis for inlet flow velocity 5 m/s.*

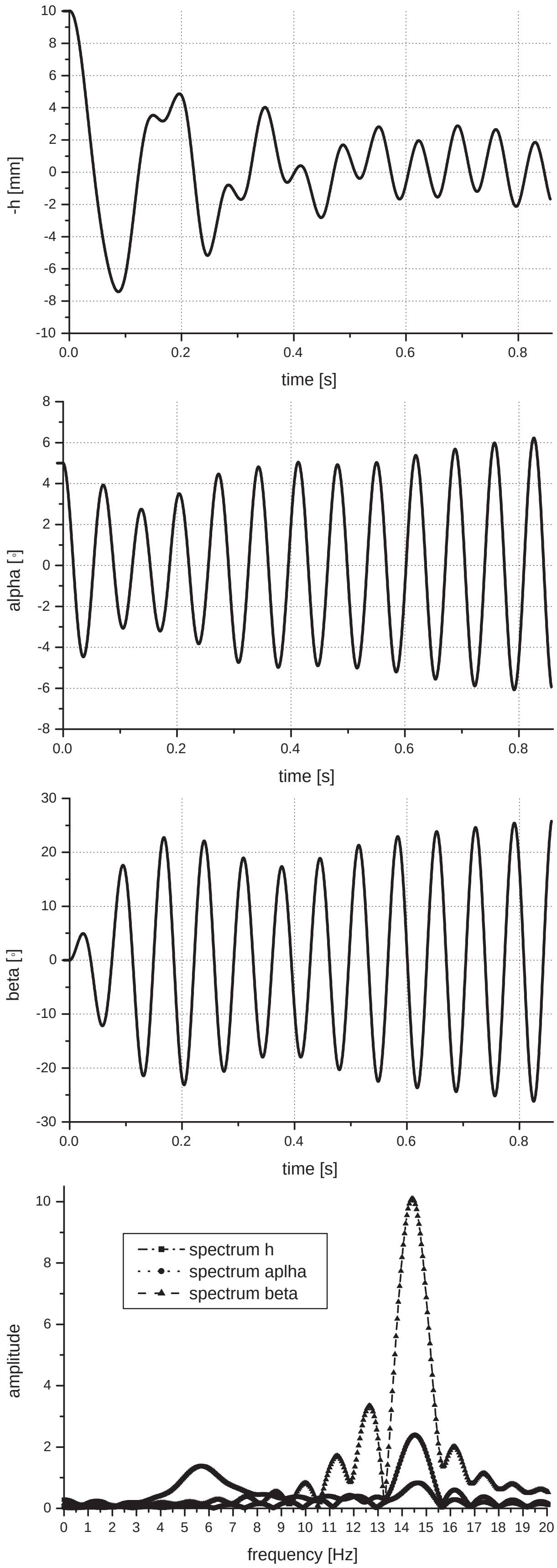

Figure 4: *Functions h, α, β and their spectral analysis for inlet flow velocity 10 m/s.*

are decreasing, the system is stable and a low level sustained vibrations are caused by vortex separation. For the higher flow velocity 10 m/s, the system is becoming unstable and rotational amplitudes of vibration are increasing in time.

7. DISCUSSION AND CONSLUSIONS

Good agreement with the NASTRAN results in the frequency analysis of the vibrations of the airfoil in dependence on increasing inlet flow velocity was obtained. Both the numerical simulations in the time domain and the NASTRAN computations show that the system becomes unstable by flutter at the inlet velocity slightly above 10 m/s. A further improvement of the computational model is possible by including the turbulence.

Acknowledgements

This research is a part of the grant No. IAA200760613 of the Grant Agency of Academy of Sciences of the Czech Republic. It was also partly supported under the Research Plans MSM 0021620839 (M. Feistauer) and 6840770003 (P. Sváček) of the Ministry of Education of the Czech Republic and the project No. 48607 of the Grant Agency of the Charles University in Prague (M. Růžička).

8. REFERENCES

Brezzi, F., Falk, R.S., 1991, Stability of higher-order Hood-Taylor methods. *SIAM J. Numer. Anal.* **28**: 581-590.

Feistauer, M., Horáček, J., Růžička, M., Sváček, P., 2008, Interaction of a flexibly supported airfoil and a channel flow. *Engineering Mechanics* (in press).

Sváček, P., Feistauer, M., Horáček, J., 2007, Numerical simulation of flow induced airfoil vibrations with large amplitudes. *J. of Fluids and Structures* **23**: 391-411.

Gelhard, T., Lube, G., Olshanskii, M. A., Starcke, J.-H., 2005, Stabilized finite element schemes with LBB-stable elements for incompressible flows. *J. Comput. Appl. Math.* **177**: 243–267.

Losík, V., Čečrdle, J., 2007, Flutter computation of 3-dof wing profile model. *Technical report P-PL-0061/07, ARTI, Prague-Letňany (in Czech).*